Two-Photon Spectroscopy of Protein-Bound Chromophores

ROBERT R. BIRGE

Department of Chemistry, Carnegie-Mellon University, Pittsburgh, Pennsylvania 15213

Received October 4, 1985 (Revised Manuscript Received March 10, 1986)

The application of two-photon spectroscopy to the study of the electronic properties of biological molecules is a relatively recent endeavor. The first two-photon spectrum of a biological chromophore was reported in 1978, and this study of vitamin A was carried out using laser equipment which is unsophisticated by today's standards.[1] Significant advances in the power, wavelength range, and reliability of tunable pulsed-dye laser systems and in the sophistication of commercially available optical and electronic signal collection equipment have dramatically improved experimental capabilities.[2] Two-photon spectroscopy is now on the threshold of becoming a routine experimental technique in biophysics. This event will have impact on a number of areas of study, because optically "forbidden" excited states are believed to be important to the biological function of many photon receptor chromophores in animals, plants, and bacteria.[3-10] Furthermore, assignment of the Franck–Condon maxima of forbidden states in protein bound chromophores can often provide unique information on the electrostatic and dispersive nature of the binding sites.[11]

The purpose of the present Account is to describe the application of two-photon spectroscopy to the study of the binding site of rhodopsin.[11] Similar experimental and theoretical techniques are being used to study the chromophore binding sites of bacteriorhodopsin,[12] 11-*cis*-retinal binding protein (CRABP),[13] superoxide dismutase,[14] chlorophyll,[15] and cytochrome C oxidase.[16] (References 12–16 provide background material and do not present two-photon spectroscopic results.) In order to appreciate the capabilities of two-photon spectroscopy, one must understand both the spectroscopic technique as well as the electronic properties of the manifold of excited states that are probed using the technique. The present discussion is therefore focused on both the theory and procedures of two-photon spectroscopy as well as the nature of the low-lying excited singlet states of the relevant biological chromophores. In order to demonstrate the global utility of this nonlinear spectroscopic technique, the application of two-photon spectroscopy to the study of porphyrins will be briefly outlined in the last section.

The Two-Photon Phenomenon

In 1931, Maria Göppert-Mayer theoretically predicted that a molecule could absorb two photons in a single quantized event.[17] This possibility represented a formerly unrecognized solution of Dirac's dispersion equation. Experimental verification of this prediction was postponed until the early 1960's and the development of the laser.

The theory of two-photon spectroscopy has been extensively reviewed[2,18-22] and the Accounts by McClain, by Hochstrasser and Trommsdorff, and by Goodman and Rava provide excellent introductions.[18] The following discussion presents the basic elements of the theory with the goal of introducing the reader to the nomenclature and the principal electronic factors that determine the probability of two-photon absorption. The interested reader should consult ref 2, 19–22 for more detailed treatments of the theory.

Theoretical Background. The allowedness of a two-photon absorption is a function both of the properties of the molecule, and the laser polarization, energy, and transverse mode structure used to generate a "simultaneous" two-photon transition in the molecule. A rough estimate of the two-photon absorptivity for a two-photon allowed state can be obtained by using the single intermediate-state (SIS approximation[2,3] along

Robert R. Birge received his B.S. from Yale University and his Ph.D. in 1972 from Wesleyan University working under the direction of the late Professor Peter A. Leermakers. After two years as a NIH postdoctoral fellow at Harvard University with Professors Martin Karplus (molecular orbital theory) and Bryan Kohler (laser spectroscopy), he joined the chemistry faculty at the University of California, Riverside, in 1975 where he initiated his studies of biological molecules using two-photon spectroscopy, laser photocalorimetry, and molecular dynamics theory. During the summer of 1984 he moved his research group to Carnegie-Mellon University where he is now Professor and Head of the Chemistry Department and Director of the Center for Molecular Electronics. An accomplished musician, Dr. Birge's compositions and arrangements have appeared on over 25 recordings.

(1) Birge, R. R.; Bennett, J. A.; Pierce, B. M.; Thomas, T. M. *J. Am. Chem. Soc.* **1978**, *100*, 1533.
(2) Birge, R. R. In *Ultrasensitive Laser Spectroscopy*; Kliger, D. S., Ed.; Academic: New York, 1983; pp 109–174.
(3) Pierce, B. M.; Birge, R. R. *J. Chem. Phys.* **1979**, *70*, 165.
(4) Birge, R. R.; Bennett, J. A.; Hubbard, L. M.; Fang, H. L.; Pierce, B. M.; Kliger, D. S.; Leroi, G. E.; *J. Am. Chem. Soc.* **1982**, *104*, 2519.
(5) Birge, R. R.; Pierce, B. M.; Murray, L. P. In "Spectroscopy of Biological Molecules"; Sandorfy, C., Theophanides, T., Eds.; Reidel: Boston, 1984; pp 473–486.
(6) Thrash, R. J.; Fang, H. L.; Leroi, G. E. *Photochem. Photobiol.* **1980**, *29*, 1049.
(7) (a) Birge, R. R.; Hubbard, L. M.; *J. Am. Chem. Soc.* **1980**, *102*, 2195. (b) Birge, R. R.; Hubbard, L. M. *Biophys. J.* **1981**, *34*, 517.
(8) Ottolenghi, M. *Adv. Photochem.* **1980**, *12*, 97.
(9) Birge, R. R. In *Biological Events Probed by Ultrafast Laser Spectroscopy*; Alfano, R. R., Ed.; Academic: New York, 1982; pp 299–317.
(10) D'Amico, K. L.; Manos, C.; Christensen, R. L. *J. Am. Chem. Soc.* **1980**, *102*, 1777.
(11) Birge, R. R.; Murray, L. P.; Pierce, B. M.; Akita, H.; Balogh-Nair, V.; Findsen, L. A.; Nakanishi, K.; *Proc. Natl. Acad. Sci. U.S.A.* **1985**, *82*, 4117.
(12) Birge, R. R. *Annu. Rev. Biophys. Bioeng.* **1981**, *10*, 315.
(13) Stubbs, G. W.; Saari, J. C.; Futterman, S. *J. Biol. Chem.* **1979**, *10*, 8529.
(14) *Superoxide and Superoxide Dismutases, Proceedings of the EMBO Workshop*, Banyuls, France, June 20–26, 1976; Michelson, A. M., McCord, J. M., Fridovich, I., Eds.; Academic: London, 1977.
(15) Eccles, J.; Honig, B. *Proc. Natl. Acad. Sci.* U.S.A. **1983**, *80*, 4959.
(16) Chan, S.; I.; Bocian, D. F.; Brudvig, G. W.; Morse, R. H.; Stevens, T. H. in Cytochrome Oxidase; King, T. E., Ed.; Elsevier/North-Holland: Amsterdam, 1979; pp 177–188.
(17) Göppert-Mayer, M. *Ann. Phys.* **1931**, *9*, 273.
(18) (a) McClain, W. M. *Acc. Chem. Res.* **1974**, *7*, 129. (b) Hochstrasser, R. M.; Trommsdorff, H. P. *Acc. Chem. Res.* **1983**, *16*, 376. (c) Goodman, L.; Rava, R. P. *Acc. Chem. Res.* **1984**, *17*, 250.
(19) (a) Friedrich, D. M.; McClain, W. M. *Annu. Rev. Phys. Chem.* **1980**, *31*, 559. (b) McClain, W. M.; Harris, R. A. In *Excited States*; Lim, E. C., Ed.; Academic: New York, 1977; Vol. 3, pp 1–56.
(20) McClain, W. M. *J. Chem. Phys.* **1971**, *55*, 2789.
(21) Peticolas, W. L. *Annu. Rev. Phys. Chem.* **1967**, *18*, 233.
(22) (a) Mortensen, O. S.; Svendsen, E. N. *J. Chem. Phys.* **1981**, *74*, 3185. (b) Dick, B.; Hohlneicher, G. *J. Chem. Phys.* **1982**, *76*, 5755.

0001-4842/86/0119-0138$01.50/0

with the potential contribution of the change in dipole moment upon excitation:[22,23]

$$\delta_{\max}^{f\leftarrow o} = \frac{8\pi^4 e^4 \tilde{\nu}_\lambda^2}{15c^2h^2} g_{\max} \left\{ \frac{(a+b)[\langle k|\mathbf{r}|o\rangle\cdot\langle f|\mathbf{r}|k\rangle]^2}{(\tilde{\nu}_k - \tilde{\nu}_\lambda)^2} + \frac{b|\langle k|\mathbf{r}|o\rangle|^2|\langle f|\mathbf{r}|k\rangle|^2}{(\tilde{\nu}_k - \tilde{\nu}_\lambda)^2} \right\} \quad (1a)$$

$$+ \frac{8\pi^4 e^2}{30c^2h^2} g_{\max} \{(a+b)S_{ab} + bS_b\} \quad (1b)$$

where

$$S_{ab} = (\mu_o\cdot\langle f|\mathbf{r}|o\rangle)^2 + (\langle f|\mathbf{r}|o\rangle\cdot\mu_f)^2 - 2(\mu_o\cdot\langle f|\mathbf{r}|o\rangle)(\langle f|\mathbf{r}|o\rangle\cdot\mu_f) \quad (2a)$$

and

$$S_b = \mu_o^2|\langle f|\mathbf{r}|o\rangle|^2 + \mu_f^2|\langle f|\mathbf{r}|o\rangle|^2 - 2\mu_o\mu_f|\langle f|\mathbf{r}|o\rangle|^2 \quad (2b)$$

where $\tilde{\nu}_\lambda$ is the wavenumber of the laser excitation, $g_{\max}$ is the maximum value of the normalized lineshape function, $\langle k|$ represents a single (one-photon allowed) intermediate state at $\tilde{\nu}_k$, a and b are photon propagation-polarization variables (see ref 3), and μ_o and μ_f are the ground- and final-state dipole moments. The above equation is a good approximation for nonpolar molecules with a low-lying, strongly (one-photon) allowed singlet state, $\langle k|$, provided the transition length $\langle f|\mathbf{r}|l\rangle$ is large. For example, the two-photon properties of the low-lying $^1A_g{}^{*-}$ state in linear polyenes are well described using the SIS approximation where $\langle k|$ is the strongly allowed $^1B_u{}^{*+}$ $\pi\pi^*$ state.[2-5] Conversely, the SIS approximation fails to accurately describe low-lying two-photon allowed states in porphyrins.[23]

An allowed one-photon transition will have a transition length of ~1 Å. A broad excitation band ($g_{\max}$ ~10^{-15} s) of a "typical" two-photon allowed state will exhibit a maximum two-photon absorptivity under linearly polarized excitation ($a = b = 8$) of ~1.7×10^{-3} $g_{\max}|\langle k|\mathbf{r}|o\rangle|^2|\langle f|\mathbf{r}|k\rangle|^2 \simeq 10^{-50}$ cm^4 sec molecule^{-1} photon^{-1}. This absorptivity value is informally known as 1Göppert–Mayer in honor of Göppert–Mayer's pioneering theoretical treatment of the two-photon absorption phenomenon.[17]

If the molecule undergoes a large change in dipole moment upon excitation into the final state, the contribution of the initial and final states, (eq 1b) can become important in determining the two-photon allowedness of both "allowed" and "forbidden" states. For example, if $|\langle f|\mathbf{r}|o\rangle|$=1 Å, $g_{\max} = 10^{-15}$ s, $|\mu_o|$ = 5 D and $|\mu_f|$ = 10 D, then term (1b) yields $\delta_{\max}$ (1b) = 0.5 GM provided μ_o, μ_f, and $\langle f|\mathbf{r}|o\rangle$ are similarly polarized. This value is only half of that predicted for a strongly two-photon allowed absorptivity indicating that one-photon allowed states can have significant two-photon absorptivities in polar compounds. If the molecule to be studied is in a polar, or highly polarizable, protein binding site, the reaction field of the environment will usually magnify the effect since $\mu_i^{\text{total}} = \mu_i + \alpha_i\mathbf{R}_{oo}$, where α_i is the polarizability of the ith state and $\mathbf{R}_{oo}$ is the ground-state protein reaction field. The sensitivity of two-photon absorptivities to the electrostatic nature of the binding site derives in part from this latter effect.

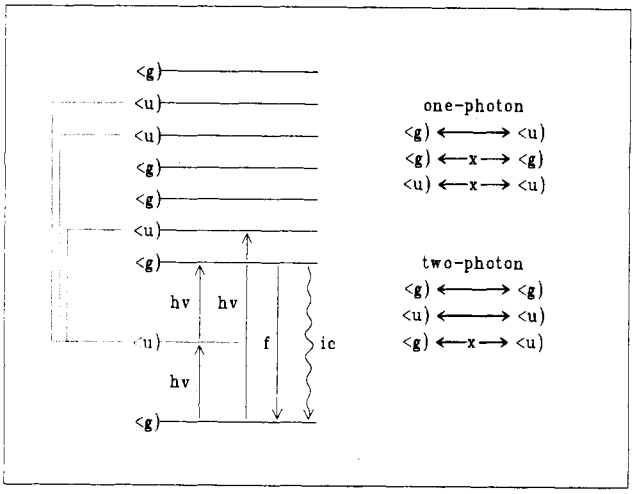

Figure 1. A two-photon transition from the ground state to the lowest-lying $\langle g|$ state is shown at the far left for a molecule with inversion symmetry. This transition proceeds via preparation of a virtual level which is a superposition of all the $\langle u|$ excited states. A second photon arrives before the virtual level decays (~10^{-15} s) to generate a final state of g symmetry. Accordingly, an allowed two-photon transition can be viewed as a sequence of two one-photon allowed transitions $\langle g|\leftarrow\langle u|\leftarrow\langle g|$ which leads to the selection rules shown at right. The final excited state returns to the ground state via fluorescence (f) and/or internal conversion (ic). If the fluorescence quantum yield is larger than 0.1, the two-photon excitation method is usually the preferred technique. Molecules with low or negligible fluorescence quantum yields can be studied using two-photon thermal lens, photoacoustic, or double resonance techniques.

One-photon transitions are allowed when the transition length has a component which transforms under x, y, or z symmetry operations. In contrast, two-photon transitions are allowed for transition-length products which have components that transform under x^2, y^2, z^2, xy, yz, or xz symmetry operations. Accordingly, Raman and two-photon spectroscopy share the same selection rules, the former accessing ground-state vibrational levels; the latter accessing excited-state vibronic levels. The selection rules for molecules with inversion symmetry are summarized in Figure 1. The complementary nature of one-photon (or infrared) and two-photon (or Raman) spectroscopy is evident, but it should be emphasized that an affirmative selection rule does not guarantee an observable transition. A $g \leftarrow g$ transition can have negligible two-photon absorptivity due to orbital overlap, or spin, restrictions. In other words, one- and two-photon selection rules describe the possibilities, but not the probabilities, of an absorption process. McClain has reviewed the two-photon selection rules for all 32 crystallographic point groups and the two linear molecule groups.[20]

Two-Photon Selection Rules in Polyenes. Linear polyenes are represented by the C_{2h} point group, and the $\pi\pi^*$ states of these molecules can be classified under one of four possible symmetries: $^1A_g{}^{*-}$, $^1A_g{}^{*+}$, $^1B_u{}^{*-}$, $^1B_u{}^{*+}$. (The superscript "+" and "–" labels derive from orbital pairing relationships as discussed below.) The ground state has $^1A_g{}^{*-}$ symmetry and couples via one-photon selection rules only with $^1B_u{}^{*+}$ states. Accordingly, the virtual state must have $^1B_u{}^{*+}$ symmetry. The second photon must access the final state by a one-photon allowed process, and therefore the final state must have $^1A_g{}^{*-}$ symmetry. Accordingly, only $^1A_g{}^{*-}$

(23) Masthay, M. B.; Findsen, L. A.; Pierce, B. M.; Bocian, D. F.; Lindsey, J. S.; Birge, R. R. *J. Chem. Phys.* **1986**, *84*, 3901.

states are two-photon allowed in linear polyenes. Retinyl polyenes belong to the C_1 point group. The fact that all electronic states have the same symmetry (A) means that all excited singlets are formally allowed in both one-photon and two-photon spectroscopy. Nevertheless, the excited singlet states of the visual chromophores maintain many of the characteristics of linear polyene excited states and it is useful to describe these states by reference to the C_{2h} point group (e.g., "$^1A_g{}^{*-}$", "$^1A_g{}^{*+}$", "$^1B_u{}^{*-}$", "$^1B_u{}^{*+}$"). The approximate symmetry classifications are given in quotation marks and are derived by correlating the properties of a given electronic state with those of the analogous state in a linear polyene of C_{2h} symmetry. In other words, "$^1A_g{}^{*-}$" should be interpreted as $^1A_g{}^{*-}$-like.

Two-Photon Selection Rules in Porphyrins. Although our primary goal in this Account is to describe the application of two-photon spectroscopy to the study of polyene chromophores, our preliminary studies of porphyrins suggest similar potential for probing binding sites. The symmetry and polarizability of the π electron system of porphyrins make the electronic states of these chromophores very sensitive to changes in the electrostatic environment.[15] This sensitivity suggests that two-photon studies of protein-bound metalloporphyrins can provide new insights into the electrostatic nature of the binding sites (see below).

It is convenient to analyze the properties of porphyrin excited states using D_{2h} as the "parent point group" regardless of actual symmetry. This approach is analogous to the use of C_{2h} as the parent group in analyzing polyene electronic structure (see above). If we assume a closed-shell ground state and restrict our analysis to $\pi\pi^*$ excited states, one-photon allowed states are restricted to B_{2u} (y polarized) or B_{3u} (x polarized) symmetry. Two-photon allowed states are restricted to A_g (x^2,y^2) or B_{1g} (xy) symmetry. A low-lying strongly two-photon allowed $^1A_g{}^{*-}$ (or $^1A_g{}^{*-}$-like) state is predicted to be present in porphyrins and this state exhibits the same sensitivity to environment as the $^1A_g{}^{*-}$ state in polyenes. Hence the potential of using two-photon spectroscopy to probe the environment of protein-bound porphyrins.

Experimental Aspects of Two-Photon Spectroscopy

There are numerous experimental methods of observing a two-photon absorption. One can, for example, directly observe the absorption event using a two-laser system.[18] This approach, however, is not recommended for photolabile biomolecules because of the extremely high light fluxes that are required. Indirect methods of observing the two-photon absorption process are usually more sensitive and certainly less destructive. These methods monitor the absorption of two-photons by observing solute emission (the excitation technique[2]), the heat produced via internal conversion (the thermal lens[24] or optical-acoustic techniques[25]) or a secondary electronic transition created in response to the absorption of two-photons (the double-resonance technique[26]). Following a brief description of the two-photon absorption process, the experimental details of selected indirect methods will be described.

The Two-Photon Absorption Process. The number of photons absorbed during a single laser pulse, $^2N_{abs}$, is given by,[2]

$$^2N_{abs} \simeq \frac{\delta_\lambda S C Z_{02}{}^{eff}[(l+1)(m+1)]^{-0.4}}{\pi W_{02}{}^2} \int_{-\infty}^{\infty} N(t)P(t)dt \quad (3)$$

where δ_λ is the wavelength-dependent two-photon absorptivity (cm^4 s molecule^{-1} photon^{-1}) (eq 1), S is the dimensionless two-photon correlation parameter ($S_{coherent} = 1$, $S_{chaotic} = 2$; $S = 1$ for laser excitation), C is the concentration of the two-photon absorber (molecule cm^{-3}), $Z_{02}{}^{eff}$ is the effective confocal distance (cm) (see ref 2), W_{02} is the beam radius at maximum focus (cm), l and m are the transverse excitation mode numbers, and $N(t)$ and $P(t)$ give the number and power (photons/s) of the laser photons at time t. The goal of two-photon spectroscopy is to measure δ_λ as a function of wavelength. The complication of this technique is that $Z_{02}{}^{eff}$, W_{02}, l, m, and NP_0 are all wavelength dependent. Transverse mode hopping, for example, can lead to large spectral errors since a TEM_{11} mode is 40% less efficient than a TEM_{00} mode. [Complex modes beyond the scope of eq 3 typically have efficiencies 70% below TEM_{00} (see ref 2).] Spatial filtering can be used to select TEM_{00} effectively eliminating this potential source of error (see Figure 2). More difficult to accommodate are changes in the pulse width and/or pulse shape which affect the integral in eq 3.[27] One must normally correct for these variations using pulse width correction factors (see below). Although $Z_{02}{}^{eff}$ and W_{02} are also wavelength dependent, if one selects TEM_{00} and uses achromatic optics, their wavelength dependence can be described adequately assuming Gaussian approximations ($Z_{02}{}^{eff} = Z_{02} = n\pi W_{02}{}^2/\lambda$, where n = refractive index of solvent). Equation 3 simplifies considerably if we assume TEM_{00}, Gaussian optics, and a Gaussian temporal profile laser pulse [$(P(t) = P_0 \exp(-4\ln 2\ t^2/\Gamma^2)$, $N = 1.06447\ P_0\Gamma$, Γ = laser pulse width]:

$$^2N_{abs} = 2^{-1/2}NP_0\delta_\lambda C(n/\lambda) \quad (4)$$

The Pulsed-Laser Excitation Apparatus. All of the experimental techniques to be discussed require pulsed-laser excitation to induce the two-photon absorption. It is therefore convenient to describe the main features of the pulsed-laser system and associated optics separately. The probability of inducing a two-photon absorption is dependent upon a number of experimental parameters which include wavelength, polarization, pulse energy, pulse width, pulse shape, and transverse excitation mode. The pulsed-laser excitation system shown in Figure 2a either controls or monitors each of the above variables. The caption to Figure 2 provides a detailed description of the various experimental components. Although the electronics and computer control equipment are not shown in Figure 2, this equipment is an essential component to the total system. Data collection techniques and instrumentation

(24) Fang, H. L.; Swofford, R. L. In *Ultrasensitive Laser Spectroscopy*; Kliger, D. S. Ed.; Academic: New York, 1983; Chapter 3, pp 221–232.

(25) Tam, A. C. In *Ultrasensitive Laser Spectroscopy*; Kliger, D. S., Ed.; Academic: New York, 1983; Chapter 1, pp 2–108.

(26) Birge, R. R. In *Spectroscopy of Biological Molecules*; Sandorfy, C., Theophanides, T., Eds.; Reidel: Boston, 1984; pp 457–471.

(27) Pierce, B. M.; Birge, R. R. *IEEE J. Quantum. Electron.* **1983**, *QE-19*, 826.

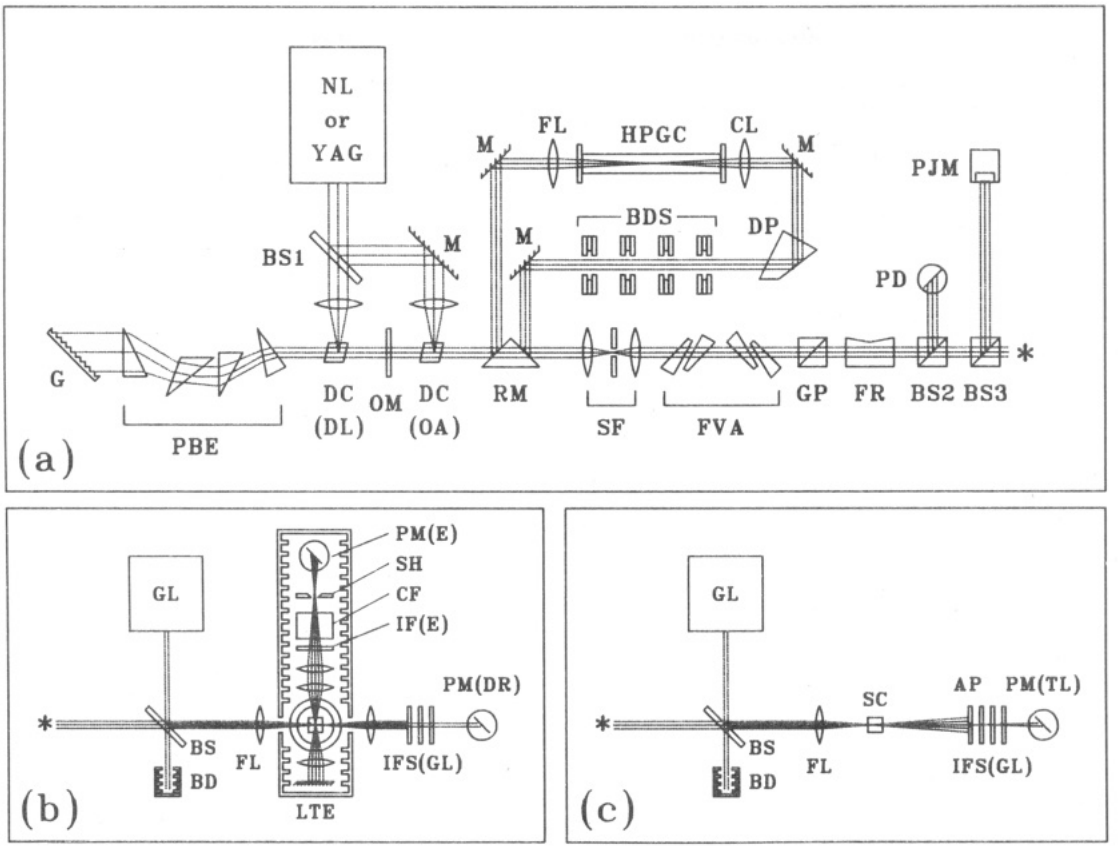

Figure 2. Principal components of our two-photon spectrometer. The pulsed-laser system is shown in (a). Apparatus to collect excitation, double resonance, and thermal lens spectra are shown in (b) and (c) and described below. A 900 KW nitrogen laser (NL) or the first or second harmonic of a Nd-YAG laser (YAG) is used to simultaneously pump two dye cells (DC) to produce optically amplified tunable dye laser excitation. A spatial filter (SF) is used to select TEM_{oo}, and a Fresnel wedge variable attenuater (FVA) is used to adjust the intensity of the laser beam. The Fresnel rhomb (FR) produces circularly polarized light or linearly polarized light depending upon angle of rotation. Two beam splitters (BS2 and BS3) direct a small fraction of the laser excitation onto a photodiode (PD) to measure pulse width and a pyroelectric Joule meter (PJM) to measure pulse energy. The Raman shifter consists of a high preessure gas cell (HPGC) containing hydrogen or deuterium and associated optics (FL, focusing lens; CL, collimating lens; DP, dispersing prism; BDS, beam dumps). The remaining symbols are: GP, glan polarizer; G, diffraction grating; PBE, prism beam expander; DC (DL), dye laser dye cell; OM, laser output mirror; BS1, dielectric beam splitter; M, dielectric mirror. Laser excitation spectra are obtained using the apparatus shown in (b) by focusing the pulsed laser radiation using an achromatic lens (FL) into the sample cell which is normally cooled to cyrogenic temperatures using a liquid nitrogen (or helium) dewar or a closed cycle helium refrigerator. Sample emission is collected perpendicular to the laser excitation by photomultiplier PM(E) [and scattered laser light is filtered out using a combination of interference (IF(E)) and chemical (CF) filters]. Thermal lens spectra are obtained using the apparatus shown in (c) using a beam splitter (BS) to combine the output of a continuous wave gas laser (GL) with the pulsed laser output to provide a colinear beam. The beam is then focused slightly in front of the sample cell (SC) using an achromatic lens (FL). A small diameter aperture (AP) passes a small fraction of laser light through three interference filters (IFS(GL)) with band passes at the wavelength maximum of the gas laser. The thermal lens signal is collected using a photomultiplier (PM(TL)) connected to a box car averager with time delayed baseline sampling capability. Double resonance spectra are obtained using the configuration shown in (b). A tunable gas laser (GL) is tuned to a transition of a state or photochemical intermediate that is populated as a result of absorption of two photons by the sample. The gas laser output is combined with the pulsed laser output using a beam splitter (BS) and the collinear beam focused into the sample. The double resonance signal is monitored by a photomultiplier (PM(DR)) after removing the pulsed laser radiation using three interference filters (IFS(GL)). Two-photon excitation and double resonance spectra can be obtained simultaneously for many samples.

are described in more detail in ref 2. The following discussions provide brief overviews of three experimental arrangements which are particularly useful for studying biological molecules.

The Two-Photon Excitation Method. The two-photon excitation technique is the method of choice for the study of forbidden states in molecules that fluoresce efficiently. This technique has been reviewed recently by Birge[2] and its application to the study of the visual chromophores is discussed in ref 5. A schematic diagram of our two-photon excitation spectrometer is shown in Figure 2, parts a and b.

A two-photon excitation spectrum is taken by monitoring the fluorescence (*f* in Figure 1) induced by the absorption of two photons by the molecule. [Note that a lowest lying one-photon forbidden, two-photon allowed state (cf. Figure 1) can still fluoresce via vibronic coupling with nearby one-photon allowed states (see ref 28 for a detailed discussion).] The number of photons emitted by the solute is nominally 5–9 orders of magnitude smaller than the number of photons in the laser excitation pulse. A combination of interference and chemical filters (IF(E), CF in Figure 2b) is often required to pass the fluorescence while preventing scattered laser light from reaching the detector.

The following equations give the two-photon absorptivity as a function of experimental observables assuming TEM_{00} laser excitation and a Gaussian temporal profile:

(28) Hudson, B. S.; Kohler, B. E. *Annu. Rev. Phys. Chem.* **1974**, *25*, 437.

$$\delta_\lambda \propto {}^2N_{em}\lambda/(NP_o) \quad (5a)$$

$$\delta_\lambda \propto {}^2N_{em}\lambda\Gamma/N^2 \quad (5b)$$

$$\delta_\lambda \propto {}^2I_{em}\lambda/[N^2g_2(\Gamma/\tau)] \quad (5c)$$

$$\delta_\lambda \propto {}^2I_{em}\lambda/[I_0{}^2f_2(\Gamma/\tau)] \quad (5d)$$

where ${}^2N_{em}$ is the photons/pulse of the detected fluorescence, λ is the laser excitation wavelength, ${}^2I_{em}$ is the intensity of the observed emission at maximum, I_o is the intensity of the laser excitation pulse at maximum, and $g_2(\Gamma/\tau)$ and $f_2(\Gamma/\tau)$ are the pulse width correction factors tabulated in ref 27.

A plot of log (S) vs. log (R) at a fixed wavelength, where S is the signal (${}^2N_{em}$ or ${}^2I_{em}$) and R is the reference (N or I_0), should yield a slope of 2 within experimental error.

The Thermal Lens Technique. The thermal lens technique is a very sensitive method of observing two-photon spectra of molecules that do not fluoresce. A schematic diagram of our two-photon thermal lens spectrometer is shown in Figure 2c. Thermal lensing arises in an irradiated liquid sample when a fraction of the laser beam is absorbed and subsequently converted into thermal energy via internal conversion back to the ground state (ic in Figure 1). The irradiated volume changes temperature radially from the beam axis, with the temperature increase being greatest on the axis. In response to the radial change in temperature there is a radial change in the refractive index in the irradiated volume. A transient "thermal lens" is formed which changes the intensity of the CW monitoring gas laser beam passing through a small aperture (AP, Figure 2c) down-field, provided the center of the sample cell is displaced from the position of maximum focus of the CW gas laser beam.

The signal, S, observed in pulsed-laser thermal lensing is $\Delta I_{bc}/[I_{bc}(t = 0)]$, where $I_{bc}(t = 0)$ is the intensity of the monitoring laser at the beam center at maximum deflection (just after the dye laser pulse has passed through the cell) and $\Delta I_{bc} = I_{bc}(t = 0) - I_{bc}(t = \infty)$, where $I_{bc}(t = \infty)$ is the base-line intensity observed after decay of the thermal lens. The two-photon absorptivity is related to the observed thermal lens signal using the following formula:

$$\delta_\lambda \propto \lambda^2 S\Gamma/N^2 \quad (6)$$

The recent review by Fang and Swofford[24] should be consulted for a more detailed discussion of the two-photon thermal lens technique.

The Double-Resonance Technique. The double-resonance technique represents one of the most sensitive methods of observing a two-photon transition. The principle is simple and requires that the solute under study undergo a wavelength independent photochemical transformation or that the solute intersystem crosses to form a metastable excited state. The probe laser then interrogates the formation of the resulting species. The application of this technique to the study of bacteriorhodopsin is discussed in ref 26.

Spectral Presentation. Spectroscopists are primarily interested in assigning the final-state vibronic distribution, and consequently two-photon spectra are normally plotted as a function of the combined energy of the two photons absorbed in accessing the final state. This convention allows for the simultaneous display of both one-photon and two-photon spectra using the same axes when studying similar vibronic regions of the molecule. It does have the disadvantage of introducing potential confusion since the laser excitation frequency used to generate the spectrum differs from the frequency displayed. All of the two-photon spectra described below were taken using a single (pump) laser source and hence the laser frequency is exactly half of the frequency marked. The vertical axis is linear in absorptivity (eq 5 and 6).

The Nature of Polyene Electronic Excited States

Hudson and Kohler's discovery of the lowest lying forbidden ${}^1A_g{}^{*-}$ $\pi\pi^*$ singlet state in diphenyl octatetraene,[28] has prompted important revisions in our understanding of polyene electronic structure.[29] It is now generally accepted that all long-chain linear polyenes possess lowest lying ${}^1A_g{}^{*-}$ $\pi\pi^*$ states and that their proper molecular orbital descriptions require a minimum configuration interaction basis set including both singly and doubly excited states.[3,4,7-9,11,12,29] Theoretical studies suggest that the interaction of the "${}^1A_g{}^{*-}$" forbidden state with the nearby strongly allowed "${}^1B_u{}^{*+}$" state is responsible for many of the unique spectroscopic and photochemical properties of polyenes and visual chromophores.[7-9] The purpose of the present discussion is to provide a brief introduction into the electronic properties of these two states with an emphasis on how environmental perturbations influence the spectroscopic properties. A basic goal of this Account is to demonstrate that the simultaneous assignment of both the "${}^1B_u{}^{*+}$" and "${}^1A_g{}^{*-}$" $\pi\pi^*$ states in protein-bound polyene chromophores provides a unique spectroscopic window on the nature of the protein environment. This observation follows from the fact that these two excited states respond very differently to changes in the electrostatic and dispersive characteristics of the environment.

The "${}^1A_g{}^{*-}$" state is frequently referred to as a "covalent" state, a reference to a valence bond description involving linear combinations of bonding diagrams that have small amounts of charge separation. The "${}^1A_g{}^{*-}$" state is characterized by a highly correlated electron configuration in which the electrons "avoid each other" effectively reducing electron repulsion. In contrast, the "${}^1B_u{}^{*+}$" state is an "ionic" state that is described in terms of bonding structures with higher degrees of charge separation and electrons tend to "pile up" in various locations along the π system. External perturbations which create an "ionic" environment will stabilize the "${}^1B_u{}^{*+}$" state and destabilize the "${}^1A_g{}^{*-}$" state (relative to the ground state). Examples of "ionic" perturbations include asymmetric substitutions, protonation, or external charges which increase the dipole moment or net absolute charge of the total system. Conversely, changes in substitution or environment which decrease the extent of the "ionic" perturbations will reverse the trend by stabilizing the covalent "${}^1A_g{}^{*-}$" state and destabilizing the "${}^1B_u{}^{*+}$" state. Examples include substituents that decrease the molecular dipole moment or external counterions which restore neutrality. The effect that protonation and/or external charges have on the relative electronic energies of the

(29) Tavan, P.; Schulten, K. *J. Chem. Phys.* **1979**, *70*, 5407.

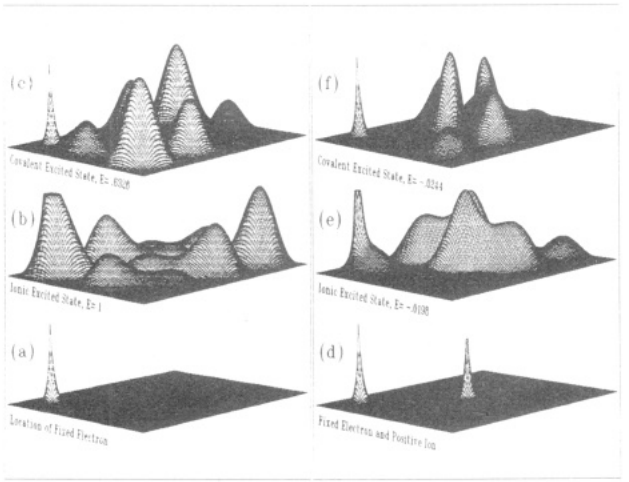

Figure 3. Particle-in-a-box wave functions for "covalent" and "ionic" excited states for two electron systems in the absence (a–c) of, and in the presence (d–f) of, a positive charge localized in the center of the box. The contours shown in (b), (c), (e), and (f) represent the wave function squared for one electron when the other electron is arbitrarily fixed in the upper-left-hand corner of the box (a). The "ionic" state is represented as an excited singlet [m = 3 (m = x axis quantum number) and n = 2 (n = y axis quantum number)]. The "covalent" state is represented as a spin coupled triplet of identical spatial quantization (see text). Note that the addition of a positive charge in the center of the box stabilizes the "ionic" state by 1.0198 energy units and the "covalent" state by 0.667 energy units.

"covalent" "$^1A_g{}^{*-}$" state and the "ionic" "$^1B_u{}^{*+}$" state can be examined from a different perspective using particle-in-a-box wave functions. Illustrative results are shown in Figure 3 where the "ionic" excited state is represented as a singlet with quantum numbers of m = 3 and n = 2 and the "covalent" excited state is represented as a singlet generated as a spin-coupled triplet–triplet double excitation of identical spatial quantization (only one of the coupled wave functions is shown). The contour heights are proportional to the square of the wave functions of one electron assuming the other is localized in the corner of the box as shown in Figure 3a. These calculations illustrate two important characteristics of "ionic" and "covalent" states. First, "covalent" states have a lower electron–electron repulsion energy because the electron motion is correlated (i.e., there is a low probability that the two electrons will occupy the same location within the box). Second, electron correlation invariably leads to a smaller stabilization energy associated with external positive charges. This latter observation follows from the fact that correlated electronic structures are intrinsically optimized to avoid electron–electron repulsion and hence an external field polarizing the electronic distribution will partially negate the relative advantages of this correlated structure. We will demonstrate below that the energy splitting between the "$^1B_u{}^{*+}$" and "$^1A_g{}^{*-}$" $\pi\pi^*$ states in the protein-bound chromophore of rhodopsin is extremely sensitive to the number and location of the external counterions.

The Visual Chromophores. The structures of various visual chromophores are shown in Figure 4. As noted previously it is convenient to describe the excited states of these polyenes using C_{2h} as the "parent point group." Thus the excited $\pi\pi^*$ states have "$^1A_g{}^{*-}$", "$^1A_g{}^{*+}$", "$^1B_u{}^{*-}$", or "$^1B_u{}^{*+}$" symmetry. The applicability of such labels varies with substitution, and in the case

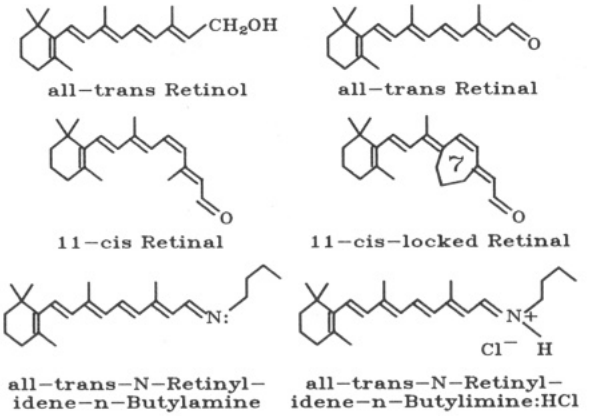

Figure 4. Structures of the visual chromophores studied using two-photon spectroscopy.

of a protonated Schiff base without a counterion (i.e., a polyene with a net charge of +1), the labels are highly approximate.

The observation of lowest lying "$^1A_g{}^{*-}$" state in linear pentaenes and hexaenes does not automatically transfer to equivalent level orderings in the visual chromophores. We will demonstrate below that the separation and the ordering of the "$^1A_g{}^{*-}$" and "$^1B_u{}^{*+}$" states is sensitive to both substitution and environment.

Two-Photon Spectroscopy of the Visual Chromophores and Rhodopsin

The level ordering of the low-lying excited singlet states of the visual chromophores has been the subject of extensive spectroscopic study and continued controversy.[8,12] The controversy is characterized by numerous conflicting assignments in the literature and is associated with the inherent difficulty of spectroscopically assigning the excited states of molecules, like the visual chromophores, which are subject to severe inhomogeneous broadening in their electronic spectra. Two-photon spectroscopy has proved to be one of the most versatile methods of studying $^1A_g{}^{*-}$-like states in such molecules.[1,4,5,11–12,30,31]

Two-photon spectra of selected visual chromophores are shown in Figure 5. The application of two-photon spectroscopy to the study of the visual chromophores has been extensively reviewed,[5,8,12,19,31] and hence our discussion will be brief. The diffuseness of the absorption and two-photon spectra precludes assignment of the system origins. Hence, level ordering is defined in terms of relative energies of the Franck–Condon maxima. This approach is not rigorously correct, and it should be noted that a lowest lying "$^1A_g{}^{*-}$" state, based on system origins, may be a second excited state based on Franck–Condon maxima (this appears to be the case for hexatrienes; see ref 32).

Two-photon excitation investigations of all-*trans*-retinol,[1] all-*trans*-retinal,[4] and the Schiff base of all-*trans*-retinal[30] indicate that all three molecules have a lowest lying "$^1A_g{}^{*-}$" $\pi\pi^*$ state in low-temperature (77 K) polar (EPA) solvent glasses (Figures 5 and 6). Since the $\pi^* \leftarrow$ n transition is "overlap" forbidden in both one-photon and two-photon spectroscopy[4], the location of the nπ^* state in all-*trans*-retinal must be inferred

(30) Murray, L. P.; Birge, R. R. *Can. J. Chem.* **1985**, *63*, 1967.
(31) Kliger, D. S. *Phys. Teach.* **1985**, *23* (Feb.), 75–80.
(32) Pierce, B. M.; Bennett, J. A.; Birge, R. R. *J. Chem. Phys.* **1983**, *77*, 6343.

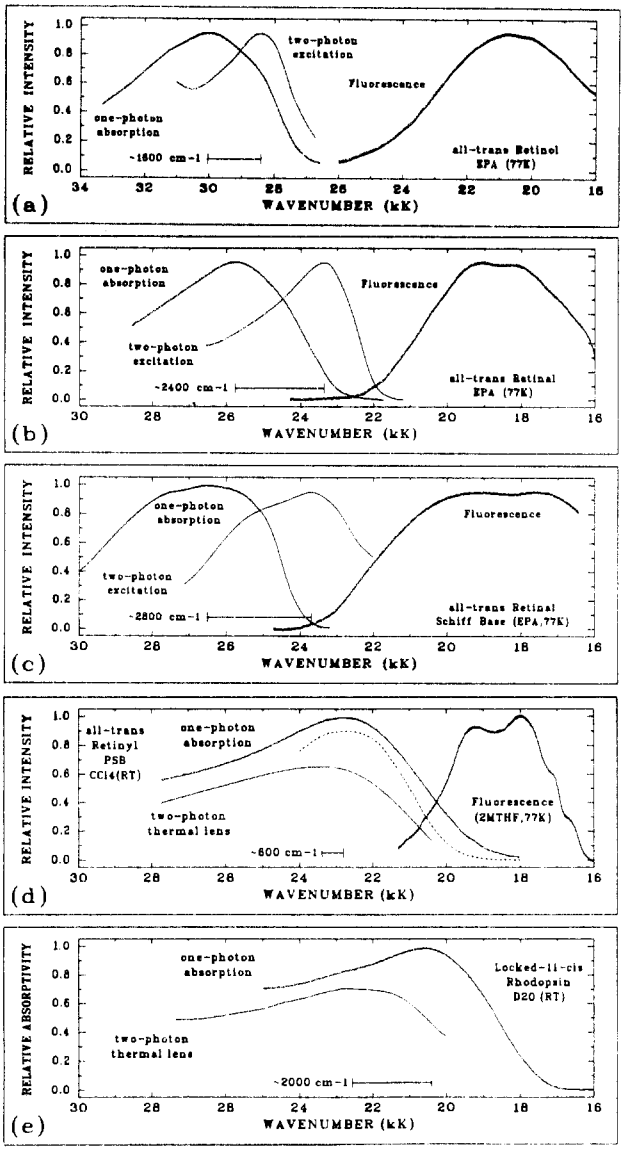

Figure 5. One-photon absorption, two-photon excitation (or thermal lens), and uncorrected fluorescence spectra of various visual chromophores in solution and a nonbleachable rhodopsin analogue containing the locked-11-*cis* chromophore. The spectra of all-*trans*-retinol (a), all-*trans*-retinal (b), and the Schiff base of all-*trans*-retinal (c) were taken in EPA (ethyl ether:isopentane:alcohol 5:5:2 v/v) at 77 K (liquid nitrogen). The one-photon absorption and the two-photon thermal lens spectra (solid lines) of the protonated Schiff base of all-*trans*-retinal (d) were taken in carbon tetrachloride at room temperature. The fluorescence spectrum, however, was taken in 2-methyl tetrahydrofuran (2MTHF) at 77 K (d). The dashed line in spectrum (d) is the one-photon absorption spectrum in 2MTHF (77 K). The spectra of the rhodopsin analogue (e) were taken in D_2O at room temperature. Note that the frequency axis in (a) is shifted and compressed relative to the corresponding axes in (b–e).

from indirect measurements. The evidence suggests that all-*trans*-retinal has a lowest-lying $n\pi^*$ state in most nonpolar solvents.[33]

Theoretical calculations predict that protonation of the retinal Schiff base will produce an ionic environment that will preferentially stabilize the "$^1B_u{}^{*+}$" state and, depending upon location of the counterion, can invert the level ordering of the low-lying $\pi\pi^*$ states.[3,7,12]

(33) Takemura, T.; Das, P. K.; Hug, G.; Becker, R. S. *J. Am. Chem. Soc.* **1978**, *100*, 2626.

(34) Honig, B.; Dinur, V.; Nakanishi, K.; Balogh-Nair, V.; Gawinowicz, M. A.; Arnaboldi, N.; Motto, M. G. *J. Am. Chem. Soc.* **1979**, *101*, 7084.

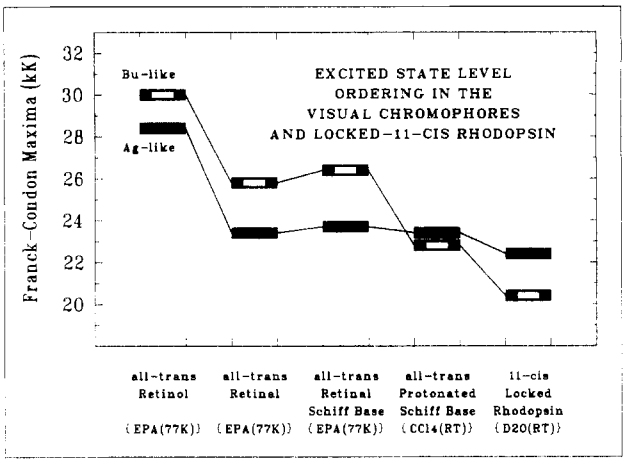

Figure 6. Comparison of the Franck–Condon maxima associated with excitation into the $^1B_u{}^{*+}$-like $\pi\pi^*$ state (one-photon absorption maxima) and the $^1A_g{}^{*-}$-like $\pi\pi^*$ state (two-photon absorption maxima) in selected visual chromophores and locked-11-*cis*-rhodopsin. The environmental conditions are described in brackets below each compound.

A two-photon study of the all-*trans*-retinyl protonated Schiff base (ATRPSB) (Figure 4) was therefore undertaken in order to test this interesting prediction. Since ATRPSB exhibits a very low quantum yield of fluorescence, the thermal lens technique was used to measure the spectrum.[11,24] The one-photon absorption and two-photon thermal lens spectra are shown in Figure 5d. Although the Franck–Condon maximum of the two-photon spectrum lies slightly above the one-photon maximum in energy, this observation does not preclude the "$^1A_g{}^{*-}$" system origin from lying below the "$^1B_u{}^{*+}$" system origin. We conclude that the "$^1B_u{}^{*+}$" – "$^1A_g{}^{*-}$" level ordering in the protonated Schiff base of all-*trans*-retinal is too close to call and is likely dependent upon solvent environment. Our results are consistent with the solution studies of D'Amico et al.,[10] and confirm the theoretical prediction that protonation preferentially stabilizes the ionic "$^1B_u{}^{*+}$" state, regardless of counterion location.

Obtaining a two-photon spectrum of the chromophore of rhodopsin provided some unique challenges. At ambient temperature, rhodopsin photobleaches under one-photon or two-photon excitation with a high quantum efficiency. The high light fluxes and signal-averaging techniques required to generate two-photon spectra prevent the use of photolabile samples. Two alternatives were investigated—the double resonance technique at reduced temperature (77 K) and the thermal lens technique using a "locked" rhodopsin analogue.[5,11] The latter method proved more reliable and was accomplished by incorporating a nonbleachable "locked-11-cis" chromophore (Figure 4) into opsin. There is compelling spectroscopic evidence to indicate that the locked-11-cis chromophore occupies the same binding site as the native 11-cis chromophore and that the counterion environment is not perturbed significantly.[11]

The Nature of the Rhodopsin Binding Site

The two-photon thermal lens maximum of locked-11-*cis*-rhodopsin is observed at 22 800 wavenumbers, ~2000 wavenumbers above the one-photon absorption maximum. We assign this thermal lens maximum to the "$^1A_g{}^{*-}$"-like $\pi\pi^*$ state which indicates that the

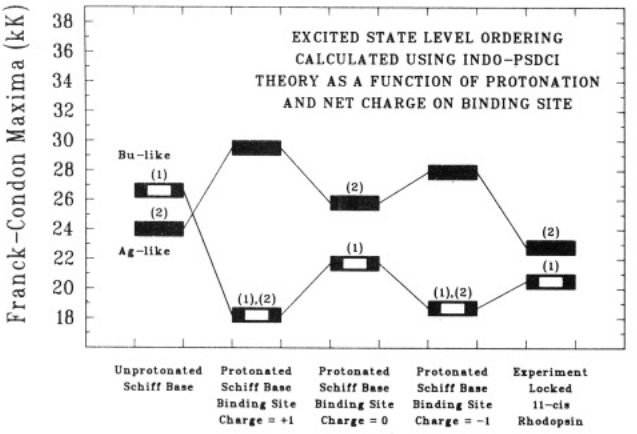

Figure 7. Comparison of calculated (INDO-PSDCI) excited state level orderings as a function of binding site model with the observed Franck–Condon maxima (locked-11-*cis*-rhodopsin). The more one-photon allowed excited state is indicated with the symbol "(1)" and the more two-photon allowed excited state with the symbol "(2)". Although a number of possibilities were investigated for each binding site model, results are reported for that calculation that yielded the closest agreement with experiment. The observation of a lowest lying $^1B_u{}^{*+}$-like state indicates that the chromophore is protonated. The prediction that the lowest lying $^1B_u{}^{*+}$-like state is more allowed under both one-photon and two-photon selection rules for charged binding sites indicates that the binding site is neutral. Note also that large "$^1B_u{}^{*+}$–$^1A_g{}^{*-}$" energy splitting predicted for the charged binding sites is not observed experimentally.

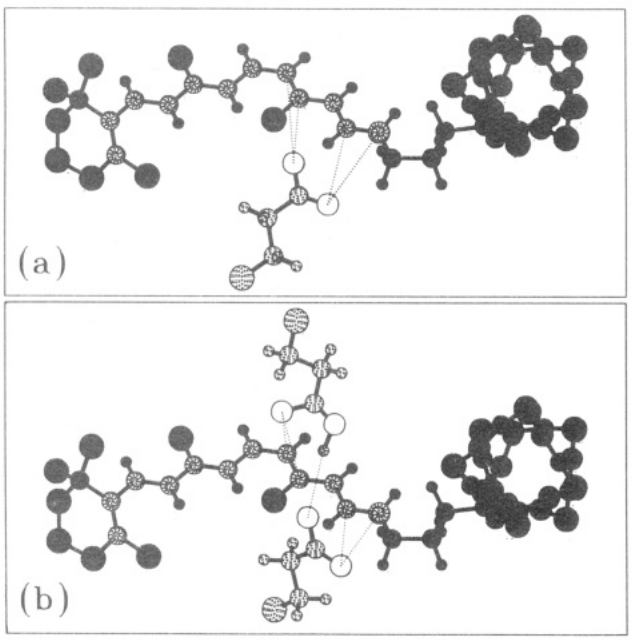

Figure 8. Two possible binding site geometries which accommodate the available one-photon and two-photon spectroscopic data. The single counterion model (a) accommodates the "two point charge model" (ref 34) by providing a single glutamic acid residue underneath the plane of the polyene chromophore. The two distinct point charges are provided by the two oxygen atoms (open circles) and the dotted lines indicate nearest atom electrostatic interactions (~3-Å separations). The two-counterion model (b) is equally capable of accommodating the available spectroscopic data and has the advantage of also rationalizing the observed deuterion isotope data (see ref 11). Note that the calculations are not sensitive to lysine geometry nor to switching aspartic for glutamic acid residues.

protein environment has induced a level ordering reversal of the low-lying $\pi\pi^*$ states relative to that observed in retinyl Schiff bases in solution (see Figure 6).

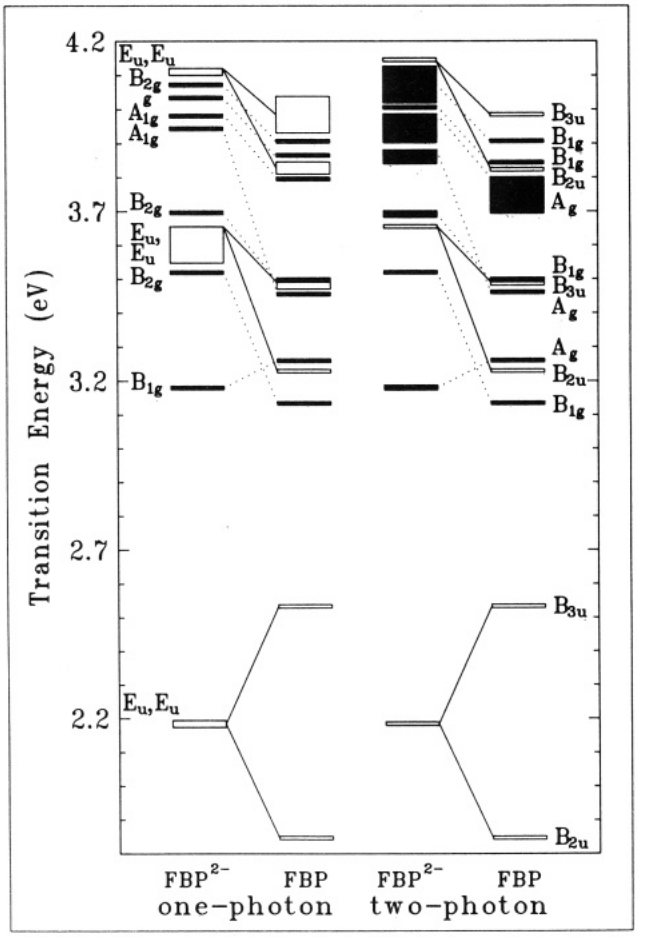

Figure 9. The $\pi\pi^*$ excited singlet states of free-base porphyrin (FBP) and its dianion (FBP^{2-}) calculated using CNDO-π-PSDCI molecular orbital theory. The vertical height of the rectangles representing the location of the excited states is proportional to the one-photon oscillator strength (left two columns) or the two-photon absorptivity for linearly polarized light (right two columns). States allowed via one-photon selection rules are indicated with open rectangles; states allowed via two-photon selection rules are indicated with solid rectangles. The CNDO-π-PSDCI calculations included all possible single excitations and all double excitations below 20 eV. The $^1A_g{}^*$ and $^1A_{1g}{}^*$ $\pi\pi^*$ states in the 3.5–4.0 eV range display sensitivity to environmental changes in a fashion analogous to the low-lying "$^1A_g{}^{*-}$" states in retinyl polyenes (see ref 23).

Comparison of the model chromophore level orderings with that observed in locked-11-*cis*-rhodopsin directly indicates that the chromophore in rhodopsin is protonated. Neither dispersive nor electrostatically induced shifts are realistically capable of inverting the "$^1B_u{}^{*+}$" and "$^1A_g{}^{*-}$" levels of an unprotonated Schiff base. Numerous test calculations using INDO–PSDCI theory substantiate this conclusion (see Figure 7). A second observation, which is somewhat more subtle, is that the binding site is neutral. INDO-PSDCI calculations demonstrate that the level ordering observed for the protein bound chromophore can be reproduced only by using a single external negative charge (or a distribution of external charges with a total charge of −1 electron units). If two negatively charged groups (total external charge of −2 electron units) are placed near the chromophore, the level separation increases (an "ionic" environment is produced) and, more interestingly, the lowest excited "$^1B_u{}^{*+}$" singlet state is more strongly allowed under both one-photon and two-photon absorption relative to the higher energy"$^1A_g{}^{*-}$" state (see

Figure 7). The level ordering separation arguments follow from the qualitative considerations described in the previous sections. A charged binding site enhances the two-photon absorptivity of the "$^1B_u{}^{*+}$" ← ← So transition due to enhancement of the initial and final state contribution to the absorptivity (eq 1b and 2). Accordingly, the chromophore in rhodopsin is protonated and occupies a neutral binding site (chromophore charge equals +1, external residue charges sum to −1).

A detailed analysis of the rhodopsin binding site using INDO-PSDCI molecular orbital theory to simulate both the one-photon and two-photon spectroscopic data leads to two possible binding site geometries as shown in Figure 8. The salient features characteristic of both models are a protonated Schiff base chromophore and one or more amino acid residues lying underneath the plane of the chromophore with a total net negative charge of −1, restoring neutrality to the binding site. Further details associated with the assignment of these two possibilities can be found in ref 11. Although not directly relevant to the present Account, it is interesting to note that the binding site model shown in Figure 8b provides a framework that has the potential of supporting a spectroscopically observable proton translocation subsequent to the primary photoisomeriazation.[11]

Prospects for the Future: Porphyrins, Chlorins, and Amino Acids

Our discussion has emphasized the use of two-photon spectroscopy to study polyene chromophore binding sites. Although the rhodopsin binding site is the only site studied to date, preliminary two-photon investigations of bacteriorhodopsin indicate that a similar approach will provide new insights into the binding site of the light adapted species of this protein. Two-photon studies of protein binding sites are not limited to those incorporating polyene chromophores, however. As shown in Figure 9, theoretical calculations indicate that the excited state manifolds of porphyrins contain low-lying covalent excited $\pi\pi^*$ states which are strongly two-photon allowed.[23] These states are predicted to respond to changes in the electrostatic environment with the same sensitivity that the "$^1A_g{}^{*-}$" states exhibit in retinyl chromophores.[23] For example, changes in the charge on the central metal atom produce spectral shifts in "ionic" and "covalent" states analogous to those observed for the simple particle-in-a-box example (Figure 3). Experimental studies are underway to verify this prediction. If experiments confirm the theoretical predictions, two-photon spectroscopy will provide a sensitive spectroscopic method of determining the location of external counterions and the net charge on the central metal atom in protein bound porphyrins and chlorins.

Polarized two-photon fluorescence excitation spectra of indole and benzimidazole have recently been obtained by Callis and co-workers.[35] These experiments have provided important new insights into the electronic structure of aromatic amino acids.[18c] The observation that indole has an unusually large two-photon absorptivity (10 times larger than the comparable transition in benzene) suggests that two-photon spectroscopy may be useful for studying the environments of selected amino acids, such as tryptophan, in proteins.[35]

It is a pleasure to acknowledge and thank my graduate students, Drs. J. A. Bennett, T. A. Cooper, L. A. Findsen, L. M. Hubbard, M. B. Masthay, L. D. Murray, and B. M. Pierce whose thesis research is described in this Account. This research was supported in part by the National Institutes of Health (EY-02202, GM-34548) and the National Science Foundation (CHE-7916336).

(35) Anderson, B. E.; Jones, R.; Rehms, A.; Illich, P.; Callis, P. R. *Chem. Phys. Lett.*, in press.